

Turbo Expander Driven Induction Generator Power Quality Improvement Using Fuzzy-PI Controlled STATCOM

Mehdi Taleshian Jelodar, *Hasan Rastegar, Hossein Askarian Abyaneh

Electrical Engineering Department, Amirkabir University of Technology, Tehran, Iran
*rastegar@aut.ac.ir

Abstract: Turbo-expanders are very useful equipment for energy recovery in gas pressure reduction stations. Using these equipment for generating electrical energy has gained more attention recently. On the other hand, turbo expander driven generators affect the electrical networks considerably as a new type of distribution power generation. To investigate the effects, first the turbo-expander is analyzed in conjunction with the electrical networks and then some power quality problems are studied in this paper. To overcome the observed problems the FACTS devices are advised. Because of the system nonlinearity, a nonlinear fuzzy –PI controller is used for the STATCOM control system. Finally behavior of the system is compared in the cases with conventional and fuzzy PI controllers. [Jelodar MT, Rastegar H, Abyaneh HA. **Turbo Expander Driven Induction Generator Power Quality Improvement Using Fuzzy-PI Controlled STATCOM.** *J Am Sci* 2013;9(6):528-536]. (ISSN: 1545-1003). <http://www.jofamericanscience.org>. 66

Keywords: Turbo-expander; distributed power generation; flexible AC transmission systems; fuzzy control

1. Introduction

The increasing need of energy sources in developing countries on one hand and new explorations of oil and gas in the oil producing countries on the other hand and also cost-effectiveness of the fossil energies has led to an increasing use of this type of energy. In this field, natural gas has become one of the most utilizable fossil energies in the world. The gas network all around the world involves hundreds of kilometers gas pipe and thousands stations for increasing or reducing gas pressure.

For long distances gas transmission its pressure should be increased in order to the size of gas pipes be reduced and also the volume of transmitted gas be increased. This is done by compressors which use a considerable amount of energy in the gas stations. On the other hand, the gas pressure should be decreased in some steps at the end of transmission lines before being delivered to the final consumers. Gas pressure reduction is normally done by some types of valves known as pressure regulating valves. What happens here is an isenthalpic process and does not produce any work. In other words when the pressure regulator valve is used, the energy contained in high pressure gas is dissipated through the expansion process and appears as turbulence and noise [1].

Gas pressure reduction can also be done by turbo-expanders. Turbo-expander is a type of turbomachineries that can be good replacement for the conventional pressure regulating valve. Replacing the regulator valves with these turbines not only causes the gas pressure to decrease when passing through the turbine, but also a large amount of the high pressure

gas energy can be recovered in the form of mechanical energy and delivered on the shaft of turbo-expander. This process in the expander turbine is almost an isentropic process [2].

Using turbo-expanders has a long history in industries which contain cooling processes, liquefaction processes, compressor driving and etc. But as electrical energy has much more benefits compared to other types of energies, a relatively new application is driving the electrical generators. In fact, easier transmission of electrical energy, high capability of being converted to the other types of energy and the ability to be used everywhere in any form, have made the electrical energy a very fascinating one. Hence, in recent years more efforts are done to use the electrical energy produced by the generators coupled with turbo-expanders. Depending on gas flow rate and pressure ratio, these systems can produce up to several mega watts power in gas pressure reduction stations [3].

2. Study System and Problem Statement

A simplified diagram of the system is shown in Figure 1. Based on this figure, high pressure gas enters the system through two paths. One is the lower path which is through the pressure regulating valve and the other is the upper path including expander turbine and some optional equipment including preheater, reheater, control valves and so on. In normal mode, the turbo-expander path is open to transmit the gas. The regulator valve can be opened every time it is required. In some systems the gas temperature is greatly reduced when it passes through the expander turbine. The low outlet gas temperature can harm the turbine, so in order to prevent vane

corrosion it is necessary to heat the gas by a preheater before entering the expander. Also, the gas temperature delivered to the consumer should be at a desired level. If it is below this level, a reheater must be used after the turbine to satisfy the condition. In order to control the opening and closure of the turbine path, a ball valve is used along with a safety trip valve to intercept the turbine path compulsively.

Some of the former studies about turbo-expanders are based on applying operational models of these systems in very small scales [4]. In these studies, usually the expander turbine is not modeled and even the turbine is studied only in the working condition by building an operational setup in small scale. Using turbo-expanders for producing electrical energy via a permanent magnet generator is investigated in [5]. In a third study, variation of the turbine parameters such as efficiency, torque and produced power is investigated

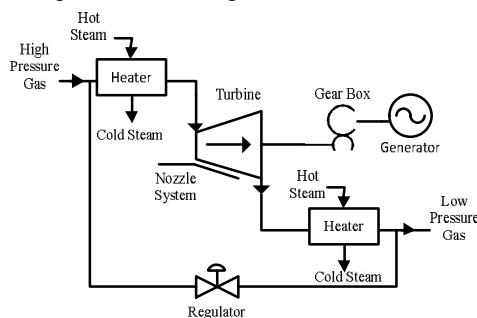


Figure 1. Simple diagram of Turbo-Expander system

An expander turbine is used beside the pressure regulator valve and an empirical analysis of the system is done in [6] and [7]. Analysis of turbo-expanders on the basis of thermodynamic fundamentals and continuity and momentum equations is presented in [8]. This study is a semi-empirical type which is about energy recovery from small heat sources in the form of mechanical energy in a cycle called Organic Rankine Cycle. A model of turbo-expander replacing the pressure regulator valve is presented in [9]. In this study, some arrangements of using this equipment coupled with the electrical generators are investigated. Then, a simple model of the expander turbine is presented regarding ideal gas and constant pressure ratio assumption across the turbine. Applying expander turbines for producing electrical energy is investigated in more details in [10]–[13] and power quality problems in various operational conditions are studied using synchronous generators. This turbo-expander is the same as the model one in [9], except that a section related to shaft and gearbox is added to the system. By adding shaft and gearbox models, the effects on transient stability of the system are investigated.

Turbo-expanders systems which drive the electrical generators in distribution voltage levels can affect the electrical energy power quality. In this paper it is focused on the turbo-expander used for driving a 9 MW induction generator in gas station of a thermal power plant and the system behavior is investigated during a momentary voltage reduction occurring on PCC (Point of Common Coupling). Since the turbo-expander is considered close to a power plant, its behavior is also investigated during starting process of the system large motors. It is shown that using FACTS device may be required to overcome the system power quality problems.

3. Turbo-Expander System Component Model

To model the system, the following assumptions are considered:

- The regulator path is closed so the gas only passes through the expander turbine.
- All the valves in the turbine path are fully opened.
- Gas temperature at the turbine inlet and outlet are at a desired level, so no preheater or reheater is needed in the system.

3.1. Expander turbine components model

3.1.1. Turbine

In the proposed system, natural gas enters the turbine whereas methane is its main component. During passing through the turbine, the gas temperature decreases and some work will be delivered on the turbine shaft. In this study, a quasi-steady turbine model is used and it is assumed that the volumes between system components are negligible. Hence the gas flow into the system is equal to the gas flow out at every instant of time, i.e., as far as the gas flow is concerned the system is in a steady state [14], [15].

$$Q_{in} \approx Q_{out} \quad (1)$$

In some previous studies on expander turbines, the turbine pressure ratio would be assumed constant and independent from its mass flow rate [9]–[11] whereas in operational turbines, this ratio changes by the mass flow rate variations [16]–[19]. A sample variation of passing gas mass flow rate versus its pressure ratio across the turbine can be seen in Figure 2. These curves are produced from the operation test done on the turbines. Because of the turbine small volume and since the turbine dynamic time constant is very small and negligible, it is supposed that pressure ratio changes immediately after a change in mass flow rate. In other words, by using these curves, the turbine pressure ratio can be determined from its mass flow rate instantaneously.

These curves depend on the turbine rotating speed and for a given pressure ratio, the mass flow

rate decreases when the turbine speed increases. In this study, where the turbine is coupled with a three phase induction generator, the deviation of generator speed in operation modes is below 5% and according to the measurements, the turbine mass flow rate changes below 1.45% in this range of speed variation [20] which can be neglected. Hence the operating curves at the speed related to generator nominal speed would be valid for the analysis.

Some analytical equations are presented too for turbine mass flow rate versus its pressure drop [22]–[24]. One of these formulae is the Stodola equation which states the amount of mass flow rate passing through a nozzle in an isentropic expansion process for a compressible ideal gas. According to this equation, the passing flow through the turbine is related to turbine input temperature and pressure of both sides. Its proportion factor can be calculated by adjusting the parameters with the operation condition.

$$Q = \frac{C_T}{\sqrt{T_1}} \sqrt{Pr_1^2 - Pr_2^2} \quad (2)$$

To calculate the amount of generated power and outgoing gas temperature, first the turbine efficiency should be calculated. The turbine efficiency varies by any change in the flow rate, input gas pressure or turbine speed. In 5% of normal speed variation, the amount of change in efficiency is below 0.75% [21]. Therefore the effect of speed variation on efficiency is neglected and the effects of the other two parameters will be investigated. Deviation of mass flow rate or gas pressure from its optimum point reduces the efficiency. So by defining the operation condition as equation (3), and considering the efficiency is varying between two minimum and maximum values, the total efficiency can be calculated from equation (4) [9]–[11].

$$O.C. = \left(1 - \left| \frac{Pr_{rated} - Pr_{in}}{Pr_{rated}} \right| \right) \times \left(1 - \left| \frac{Q_{rated} - Q_{in}}{Q_{rated}} \right| \right) \quad (3)$$

$$\eta_{total} = O.C. \times (\eta_{ub} - \eta_{lb}) + \eta_{lb} \quad (4)$$

The ideal work which is generated by the turbine is calculated by the equation $W = Q_1 \times \Delta h$. Considering the equations of ideal gas and writing Δh versus temperature difference, the produced work can be calculated as equation (5) [2], [5], [12].

$$W = Q_1 \times \eta \times C_p \times T_1 \times \left(1 - \left(\frac{Pr_2}{Pr_1}\right)^{\frac{k-1}{k}}\right), \quad k = \frac{C_p}{C_v} \quad (5)$$

3.1.2. Variable Nozzle System

The main component which implies a dynamic on the expander turbine model is the variable nozzle system. Variable nozzle system comprises of some movable blades which can affect the turbine or fluid properties by continuous opening and closing.

Opening vane of the nozzles is automatically adjusted by a control system, based on the proposed system variable which is necessary to be regulated. The desired control system variable may be any of the following variables: output gas pressure, output gas temperature or produced work.

Turbo-expanders nozzles usually have pneumatic actuators. This system has two separate chambers which are isolated by a diaphragm. Moving this diaphragm up or down causes the nozzles enveloping ring to rotate via the lever connected to this diaphragm, and thus open or close the nozzles [25]. The lower chamber pressure is equal to atmosphere pressure and the upper chamber pressure which is controlled by a servo valve, is directly proportional to the desired nozzle angle.

Complete equations of nozzle actuator system are presented in [25]. The final transfer function which defines the change of diaphragm level versus the upper chamber pressure is according to equations (6) to (8). The diaphragm level, x_d , is related to the nozzle angle by a linear equation.

$$Pr_{act} = k_0 \theta_{error} \quad (6)$$

$$\frac{d^2}{dt^2} x_d = -\frac{K_{sm}}{M_d} x_d - \frac{B_d}{M_d} \frac{d}{dt} x_d + \frac{A_d}{M_d} Pr_{act} \quad (7)$$

$$\theta_{nozzle} = k_1 x_0 + k_2 \quad (8)$$

Since the turbine analysis is based on operational curves, the test results of different nozzle angles can also be used as the basic curves for simulation of turbine operation at different nozzle angles. Figure 2 shows variations of mass flow rate versus the turbine pressure ratio at different nozzle angles.

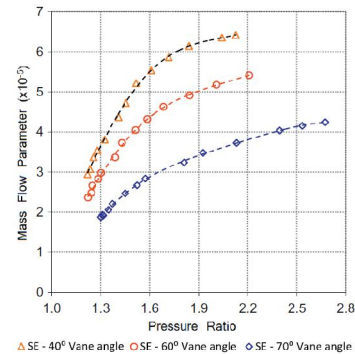


Figure 1. Mass flow rate variation versus pressure ratio for different nozzle angles [21]

When the nozzle angle increases, the coefficient C_T in equation (2) will decrease. To apply the effect of nozzle angle variation in the turbine basic equation, the coefficient C_T is explained as a function of the nozzle angle in the form of K_T/θ .

Output pressure reduction due to nozzle angle increment can be modeled by this equation.

3.1.3. Nozzle Control Logic

The nozzle control system is supposed to act on expander nozzle angle in order to stabilize the output pressure. This mechanism also affects output temperature and the power generated by the coupled electrical generator.

In this study, the control system is proposed to stabilize turbine output pressure by a proportional-integral (PI) controller on a predetermined value. So,

$$\theta_{error} = K_p (Pr_{ref} - Pr_2) + K_I \int (Pr_{ref} - Pr_2) dt \quad (9)$$

Using θ_{error} from equation (6), Pr_2 from equation (2) and θ from equation (8), the third state equation can be found as (10).

$$\frac{d}{dt} Pr_{act} = K_0 K_I Pr_{ref} - K_0 (K_I + K_P \frac{d}{dt}) \sqrt{Pr_1^2 - \frac{Q_1^2 T_1}{(K_T / (k_1 x_d + k_2))^2}} \quad (10)$$

A simple diagram of expander turbine with nozzle control system and actuator is shown in Figure 3.

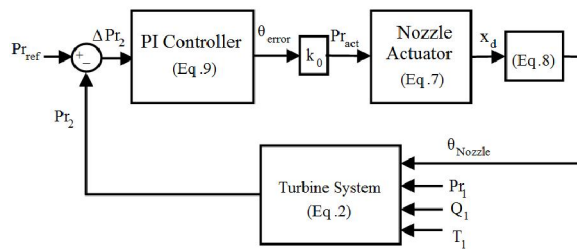


Figure 2. Turbo-expander control system diagram

3.2. Shaft and Gearbox

Usually turbo-expanders rotation speed is very high. For example, the turbo-expander of Neka power plant rotates at 23500 rpm. At this rotation speed, frequency of generated voltage would be very high and in order to avoid necessity of using power electronic converters, the rotation speed is required to be lessened by a gearbox.

The proposed gearbox is considered with transfer losses and low speed and high speed shafts are modeled by two inertias. It should be mentioned that all dampings are neglected and this is the worst-case scenario in transient stability and torsional oscillations studies. Considering the above assumptions, we have [14]:

$$n = \frac{n_l}{n_h}, J_l = \frac{J_h}{n^2}, k_l = \frac{k_h}{n^2} \quad (11)$$

$$\dot{\omega}_l = \frac{P_l - n \cdot \tau_l}{J_l + J_h} \quad (12)$$

$$\dot{\tau}_l = \frac{K_h(\omega_l - \frac{\omega_l}{n}) + B_h(\dot{\omega}_l - \frac{\dot{\omega}_l}{n})}{n} \quad (13)$$

$$\dot{\omega}_l = \frac{\tau_l - \tau_m}{J_l} \quad (14)$$

$$\dot{\tau}_m = K_l(\omega_l - \omega_{mb} S) + B_l(\dot{\omega}_l - \omega_{mb} \dot{S}) \quad (15)$$

3.3. Generator Model

The studied generator is a three phase induction generator with squirrel cage rotor. The electrical model of this generator is a fourth order state space model and the mechanical part is modeled by a constant inertia and a damping factor [26]. The motor used in the simulation is modeled in the same way.

4. Expander Turbine Model Validation

The experimental tests in [6] are used for verifying the presented model. In this empirical analysis, an expander turbine is applied in addition to the existing pressure regulator valve in an air conditioner system. The turbine is coupled with a permanent magnet generator to recover the power in the form of electrical energy. The experimental setup consists of some apparatus, among which the nozzle, turbine and generator are simulated. The nozzle angle in the experimental system is fixed at 65°. The flowing gas is HFC134a and in normal operation it passes through the pressure regulating valve. After 994 seconds, the regulator valve closes completely and the gas is transmitted into the turbine path immediately. For model validation, the mass flow rate of the turbine is reconstructed from the experimental data as shown in Figure 4. The model experiences a 0.25 kg/s step change in the mass flow rate.

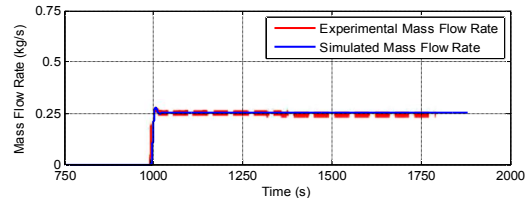


Figure 3. Experimental and simulated mass flow rate

The input pressure and temperature of the gas entering the turbine are 14.7 bar and 320°K, respectively. Variation of input and output pressures are shown in Figure 5 for both the experimental and simulated systems. The simulation results show a good compatibility between the measured and simulated pressures of the output flow.

Another important parameter investigated in the experimental system is the coupled generator voltage variation when the output power changes. Figure 6 demonstrates variation of the generated voltage during variation in the output power. The generator power is changed by an electrical load variation. Simulation results have a good compatibility with the experimental results, where the maximum deviation from the measured speed and voltage values is approximately 2.8%.

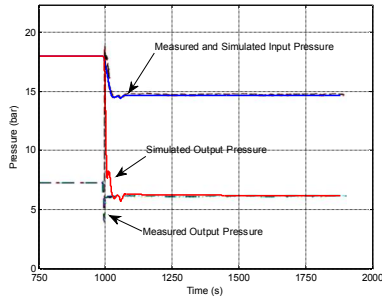


Figure 4. Measured and simulated input and output pressures

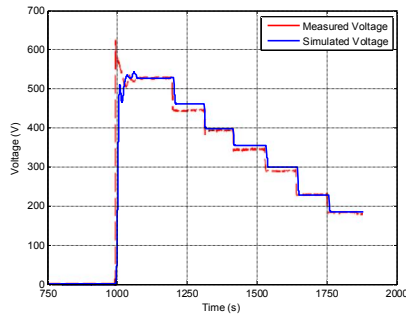


Figure 5. The generator measured and simulated voltage

5. Study System

The studied system is shown in Figure 4. This system includes an expander turbine, gearbox and an induction generator that is connected to a 20 kv network. The system load involves some static loads and a 4 MW motor load. In this section the system behavior is studied under various disturbances.

5.1. System Behavior during Momentary Input Gas Pressure Reduction

Input gas pressure may have some random variations which are implied by the consumer or by the system control or protection equipment. Although all the variations cannot have great effects on the system, in some cases it may lead to a situation in which the system forced to work in an improper condition. To show this condition, a momentary turbine input pressure drop is simulated. The momentary input pressure reduction at constant

passing flow can cause the output pressure decrement to very low values according to equation (2). At the same time, the output gas temperature decreases to the lower levels in comparison with the normal condition. It results in an increased output power and affects the coupled induction generator rotating speed. To show this, a short time input gas pressure reduction is simulated at $t=0.4s$, from 19 bar to 8.54 bar for duration of 0.7s. When the input pressure decreases, the output pressure reaches a low level of about zero and simultaneously, the output power increases to high levels of about 2.15 pu.

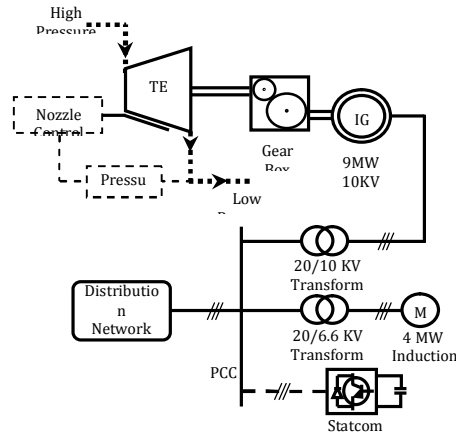


Figure 6. Studied system

When the turbine output power increases, the coupled induction generator speeds up fast and it draws very high values of reactive power from the network which causes the voltage at PCC to decrease. Due to the PCC voltage reduction, speed of the motor connected at this point decreases and draws more current from the network. If there is no FACTS device in the system, requested reactive power increment and voltage reduction are so high that both the induction generator and motor pass from their critical speed in the torque-speed diagram and hence the whole system will be unstable. Figure 8 shows the generator speed, the motor speed and the PCC voltage in this condition.

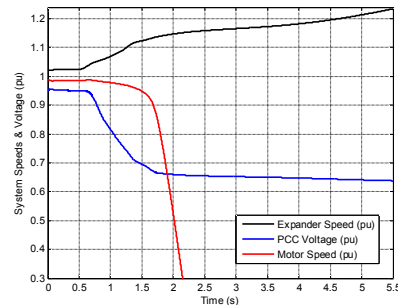


Figure 7. System quantities when a momentary input pressure reduction occurs

5.2. Using FACTS Device

The most frequently used FACTS device is the static compensator (STATCOM), being most simple, economical, and with a very fast dynamic response. To overcome the power quality problem and increasing the system stability, a 15 MVA STACOM is used at the electrical network 20 KV bus. The STATCOM basic equations are [27]:

$$L \frac{di_d}{dt} = -Ri_d + \eta_d v_{dc} - v_d \tag{16}$$

$$L \frac{di_q}{dt} = -Ri_q + \eta_q v_{dc} - v_q \tag{17}$$

$$C_{dc} \frac{dv_{dc}}{dt} = -\frac{3}{2}(\eta_d i_d + \eta_q i_q) - \frac{v_{dc}}{R_L} \tag{18}$$

Where i_d, i_q, v_d and v_q are currents and voltages at the ac side in the d-q reference frame, η_d and η_q are control signals, and v_{dc} is the dc voltage. The parameters R and L stand for resistance and inductance in the coupling transformer, C_{dc} is the capacitor in the dc-bus, and R_L represents the equivalent converter losses. The equations describing the STATCOM are nonlinear because of the products between control and state variables. The STATCOM control system has two AC and DC voltage regulators and two current regulators for d-q axis currents. Current control loop is shown in Figure 9 and complete equations of the system are presented in [27]. Conventional PI controllers are considered for the regulators and because of the system nonlinearity, a fuzzy-PI controller is also designed for current regulators and the results are compared.

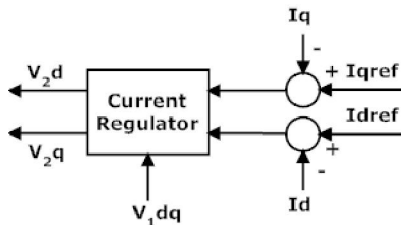


Figure 8. Current control loop of proposed STATCOM

5.3. FUZZY Proportional Integral Controller (FPIC)

The PI type of fuzzy logic controller is known to be relatively simple to implement and performs very well in first order systems [28]-[30]. The continuous-time non-fuzzy or conventional PI controller is described as:

$$u(t) = K_p e(k) + K_I \int e(k) dt \tag{19}$$

where $u(t)$ is the plant control signal at time t , $e(t)$ is the difference (error) between the desired plant

output (the set point) and the actual value, K_p is the proportional gain, and K_I is the integral gain. In order to implement the conventional PI controller digitally, (19) must be expressed in its discrete-time form, which is

$$\Delta u(k) = K_p \Delta e(k) + K_I e(k) \tag{20}$$

where $\Delta u(k)$ is the plant control input increment for the next time interval, i.e.,

$$u(k+1) = u(k) + \Delta u(k) \tag{21}$$

and $u(k)$ and $u(k+1)$ are respectively, values of the plant control input at the current and subsequent sampled times. Also, $e(k)$ in (20) is the error between the desired and actual plant outputs at the current time sample. As it can be seen in Figure 10 for currents in d (and q) axis:

$$e(k) = i_{d-ref}(k) - i_d(k) \tag{22}$$

$\Delta e(k)$ in (20) is the difference between the current and previous errors, i.e.

$$\Delta e(k) = e(k) - e(k-1) \tag{23}$$

The fuzzy (rather than conventional) PI controller is a velocity type controller in which the incremental control output given by (20) is replaced with

$$\Delta u(k) = F(K_p \Delta e(k), K_I \Delta e(k)) \equiv \Delta u_F(k) \tag{24}$$

for the conventional case, where $F(\dots)$ is a nonlinear fuzzy function. Thus, (21) can be rewritten as

$$u(k+1) = u(k) + F(K_p \Delta e(k), K_I \Delta e(k)) \equiv \Delta u_F(k+1) \tag{25}$$

The current regulator FPIC uses (24) and (25) to generate incremental control of phase voltage from the error and the change of error between i_{dq} and i_{dq-ref} . Figure 10 illustrates the basic FPIC with its four constituent components, i.e., the fuzzifier, rule base, inference engine, and defuzzifier.

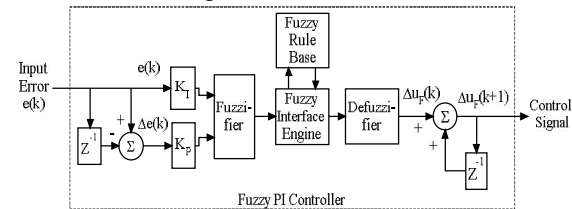


Figure 9. Fuzzy PI controller (FPIC)

Each the fuzzy controller input is normalized for the possible operating range between -1 and 1 based on the nominal values. Then the inputs and the output are classified into five levels as “Big Negative”, “Small Negative”, “Zero”, “Small Positive” and “Big Positive”. Membership functions for the current controller are shown in Figure 11. In the present study a Mamdani type is selected as the fuzzy controller. Designed rules for this controller are listed in Table 1.

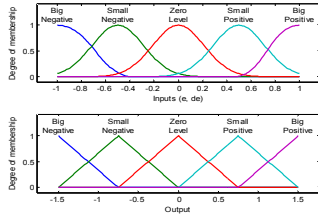


Figure 10. Membership functions of fuzzifier input and output variables e and Δe

Table 1. Fuzzy rule table

e Δe	LN	SN	Z	SP	LP
LN	LN	SN	Z	Z	SP
SN	SN	Z	SP	SP	LP
Z	SN	Z	SP	LP	LP
SP	SN	Z	SP	LP	LP
LP	SN	SP	LP	LP	LP

5.4. System Behavior with STATCOM During Momentary Input Gas Pressure Reduction

In this section, a disturbance similar to the one described in section A is applied to the expander. Because of the STATCOM in this system, the system remains in a stable mode when the input pressure comes back to its nominal value. Figure 12 shows the expander speed for three cases. The first curve belongs to the system without STATCOM, as shown in Figure 8. The other curves belong to the expander speed in the case of conventional and fuzzy PI controllers of the STATCOM. Figures 13 and 14 show the PCC voltage and the motor speed in these three cases.

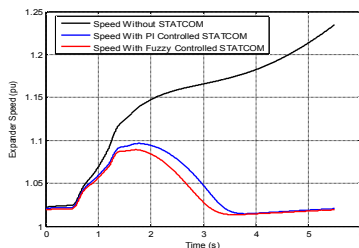


Figure 11. Expander (generator) speed

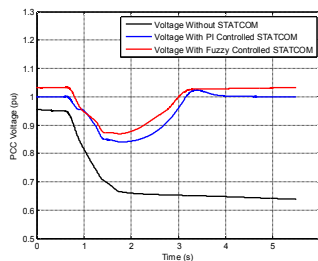


Figure 12. Voltage of PCC during and after input pressure disturbance

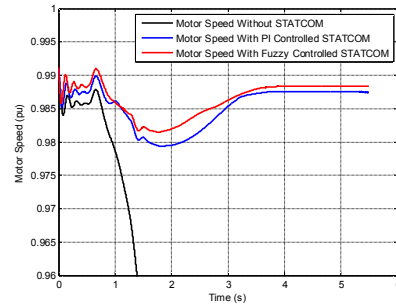


Figure 13. Motor speed during and after input pressure disturbance

In the cases that the STATCOM added to the system, some reactive power is supplied to the system even in normal condition and the voltage at PCC is stabilized at a higher level, although this is not the aim of using this device. Adding the STATCOM to the system causes the generator and motor to be stable during turbo-expander output power change. Using both PI or fuzzy controller for STATCOM causes the system to remain stable, but as can be seen in the figures, by the fuzzy controller, the voltage at PCC is at a higher level than the case with PI controller and the maximum speed of the induction generator during these variations is lower compared to the PI controller case. These results show the STATCOM with the fuzzy controller has a better behavior than the case with PI controller.

5.5. System Transient During Starting Second Turbo-expander

The system induction generator has relatively high power. Starting this generator from zero speed takes a long time and draws a high value of reactive power. In operational turbo-expander systems, the peak of drawn reactive power is recorded about tens of MVAR. This value of reactive power during the startup can cause the voltage to drop at PCC and the system motors or generators to stall under this voltage drop.

To avoid this condition in the operational systems, the generator is derived by the turbo expander until it reaches to the speeds of about 0.95 pu and then at this instant the generator circuit breaker will close. Starting by this method restricts the transient oscillations of the generator, but it still draws a high level of reactive power when connects to the network and causes the big voltage sags to occur at PCC. By adding the STATCOM to the system, the drawn reactive power from the network decreases and so, the voltage sag at the PCC will be restricted.

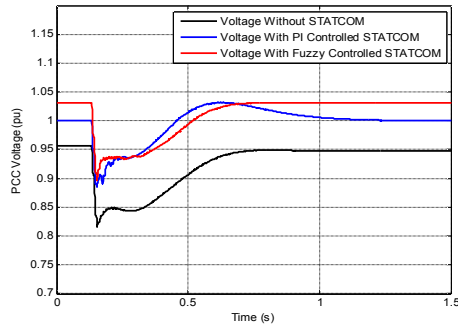


Figure 14. PCC voltage with and without STATCOM

PCC Voltage during the second generator startup is shown in Figure 15. It can be seen that using the STATCOM has improved the voltage profile during and after startup process. About 1.15 second after the startup without STATCOM, the system reaches the steady state. This time decreases to about 0.6 second when the STATCOM is used.

6. Conclusion

The expander turbine driven generators are introduced as a new type of distributed generation in this paper. After describing the turbo-expander system components, the system behavior is studied in some conditions involving two disturbances in the system mechanical and electrical parts. In the mechanical section a momentary pressure drop is considered for expander turbine input and in the electrical field a second turbo-expander driven generator startup is considered as the disturbance. Both of the disturbances cause such a condition that a considerable amount of reactive power will be drawn from the network and will be led to a voltage drop that can force the generators or motor loads to stall under these conditions. To overcome the problem, using STATCOM is advised because of its being the simplest, most economical, and with a very fast dynamic response. To have a better control in this nonlinear system, it is shown that a fuzzy-PI controller can improve the system status better than a conventional PI controller.

Corresponding Author:

Hassan Rastegar
Electrical Engineering Department
Amirkabir University of Technology
Tehran, Iran
E-mail: rastegar@aut.ac.ir

References

1. Wojciech J, Kostowski, Usón S. Thermo-economic assessment of a natural gas expansion system integrated with a co-generation unit. *Applied Energy* 2013;101:58–66.

2. Heinz P. Bloch, Claire Soares. *Turboexpander and Process Applications*. Gulf Professional Publishing, Boston, 2001.
3. Daneshi H, Zadeh KH, Choobari LA. Turboexpander as a distributed generator. *Power and Energy Society General Meeting - Conversion and Delivery of Electrical Energy in the 21st Century*, 2008;1–7.
4. Peirs J, Reynaerts D, Verplaetsen F. A microturbine for electric power generation. *Sensors and Actuators A* 2004; 113, 86–93
5. Krähenbühl D, Zwyssig C, Weser H, Kolar JW. Theoretical and experimental results of a mesoscale electric power generation system from pressurized gas flow. *IOP Publishing, Journal of Micromechanics and Microengineering* 2009;19(9):1-7.
6. Cho SY, Cho CH, Kim C. Performance characteristics of a turbo expander substituted for expansion valve on air-conditioner. *Experimental Thermal and Fluid Science* 2008; 32(8): 1655-65
7. Quoilin S, Lemort V, Lebrun J. Experimental study and modeling of an Organic Rankine Cycle using scroll expander. *Applied Energy* 2010;87(4):1260–68.
8. Lemort V, Quoilin S, Cuevas C, Lebrun J. Testing and modeling a scroll expander integrated into an organic rankine cycle. *Applied Thermal Engineering* 2009;29(14-15):3094–102.
9. Maddaloni DJ, Rowe MA. Natural gas exergy recovery powering distributed hydrogen production. *International journal of hydrogen energy* 2007;32(5):557-66.
10. Turkemani MB, Rastegar H. Modular modeling of turbo-expander driven generators for power system studies. *IEEJ Transactions on Electrical and Electronic Engineering* 2009;4(5):645-53.
11. Turkemani MB, Rastegar H. Flicker assessment of turbo-expander driven synchronous generator in power distribution network. *Journal of Iranian Association of Electrical and Electronics Engineers* 2010;7(1):53-9.
12. Taleshian M, Rasregar H, Askarian H. Modeling and power quality improvement of turbo-expander driving an induction generator. *International Journal of Energy Engineering* 2012;2(4):131-7.
13. Rahman MM. Power generation from pressure reduction in the natural gas supply chain in bangladesh. *Journal of Mechanical Engineering* 2010;41(2):89-95.
14. Winterbone DE, Munro N, Lourtie PMG. A preliminary study of the design of a controller for an automotive gas turbine. *Transactions of the ASME* 1973;95(3):244-50.
15. Pagiaslis J. A digital simulation of an automotive-type gas turbine. MSc. Thesis, University of Manchester, 1971.
16. Rajoo S, Botas RM. Variable geometry mixed flow turbine for turbochargers: an experimental study. *International Journal of Fluid Machinery and Systems* October-December 2008;1(1):155-68.
17. Liangjun H, Yang C, Harold S, Jizhong Z, Mingchia L. Numerical analysis of nozzle clearance's effect on turbine performance. *Chinese Journal of Mech. Engineering* 2010;4: 1-8.

18. Haglind F, Elmegaard B. Methodologies for predicting the part-load performance of aero-derivative gas turbines. *Energy* 2009;34(10):1484–92.
19. Serrano JR, Arnau FJ, Dolz V, Tiseira A, Cervello C. A model of turbocharger radial turbines appropriate to be used in zero- and one-dimensional gas dynamics codes for internal combustion engines modeling. *Energy Conversion and Management* 2008;49(12):3729–45
20. Karamanis N, Martinez-Botas RF. Mixed flow turbines for automotive turbochargers: steady and unsteady performance. *IMEchE Int. J. Engine Research* 2002;3(3):127-38.
21. Romagnoli A, Martinez-Botas RF, Rajoo S. Steady state performance evaluation of variable geometry twin-entry turbine. *International Journal of Heat and Fluid Flow* 2011;32(2):477-89.
22. Haglind F. Variable geometry gas turbines for improving the part-load performance of marine combined cycles – gas turbine performance. *Energy* 2010;35(2):562-70.
23. Cooke D H. On prediction of off-design multistage turbine pressures by stodola's ellipse. *Transactions of the ASME* 1985;107(3):596-606.
24. Chaibakhsh A, Ghaffari A. Steam turbine model. *Simulation Modelling Practice and Theory* 2008;16:1145-62.
25. A Mehmood A, Laghrouche S, Bagdouri M. Modeling identification and simulation of pneumatic actuator for VGT system. *Sensors and Actuators A: Physical* 2011;165(2):367-78.
26. Krause PC. *Analysis of Electric Machinery*. McGraw-Hill, 1986, Section 12.5.
27. Leon AE, Solsona JA. Software sensor-based STATCOM control under unbalanced conditions. *IEEE Transactions on Power Delivery* 2009;24(3):1623-32.
28. Kirawanich P, O'Connell RM. Fuzzy logic control of an active power line conditioner. *IEEE Transactions on Power Electronics* 2004;19(6):1574-85.
29. Alfi A, Razavi SE, Hassannia A. GA-Based Fuzzy State Feedback Controller applied to a Nonlinear Power System. *am* 2012; 8(1):313-20;
30. Ananthamoorthy NP, Baskaran K. Performance Analysis of PMSM Drive Using Intelligent Hybrid Fuzzy Controller. *life* 2012;9(1):112-20.

Appendix A. Nomenclature

A	area
B	damping constant
C_p	specific heat capacity at constant pressure (kJ/kg K)
C_v	specific heat capacity at constant volume (kJ/kg K)
F	turbine constant
H	inertia constant

h	enthalpy
i	current
J	inertia
k	spring constant
m	mass
Q	mass flow rate
n	gearbox ratio
O.C.	operating condition
P	power
Pr	pressure
R	resistance
S	generator slip
T	temperature
τ	torque
V	voltage
W	Work
X	reactance
x_d	diaphragm displacement
η	turbine efficiency
Δ	Delta
θ	angle
sm	spring (+membrane)
ub	lower band
Indices:	
1	Input
2	output
act	actuator
d	diaphragm
h	high speed
l	low speed
lb	lower band
sm	spring (+membrane)
ub	lower band

Appendix B. Simulation Parameters

Induction Generator Data:

$P_n = 9$ MW; $Z_S = 0.005 + j0.1014$ pu;
 $Z_R = 0.0178 + j0.1521$ pu; $X_m = 3.894$ pu; $H = 3.5$ s;
 $F = 0.2$ pu; Pole Pairs = 2;

Turbine data:

$P_n = 10$ MW; Nominal Speed = 23400 rpm;
 Input Pressure = 19 bar; Output Pressure = 5.2 bar;
 $\eta_{lb} = 0.7$; $\eta_{ub} = 0.85$; Input Temperature = 341 °K;
 $\dot{m} = 59.1$ kg/s

Shaft & gearbox data:

$J_H = 4$ kg m²; Gear Ratio = 1/15.6; $K_H = 30$ N/rad;
 $B_H = 800$ Ns/rad; Efficiency = 0.95;

Nozzle system data:

$A_d = 0.003$ m²; $m_d = 0.63$ kg; $b_d = 206$ Ns/rad;
 $k_{sm} = 12850$ N/rad; $k_0 = 2146.8$ rad/m;
 $k_1 = 0$ rad; $k_2 = 2000$ bar/rad;